TECHNICAL SPECIFICATION

ISO/TS 6336-22

First edition
2018-08

Calculation of load capacity of spur and helical gears —

Part 22: Calculation of micropitting load capacity

Calcul de la capacité de charge des engrenages cylindriques à dentures droite et hélicoïdale —

Partie 22: Calcul de la capacité de charge aux micropiqûres

Reference number
ISO/TS 6336-22:2018(E)

ISO copyright office
CP 401 • Ch. de Blandonnet 8
CH-1214 Vernier, Geneva
Phone: +41 22 749 01 11
Fax: +41 22 749 09 47
Email: copyright@iso.org
Website: www.iso.org

Published in Switzerland

Contents

Page

Foreword

ISO (the International Organization for Standardization) is a worldwide federation of national standards bodies (ISO member bodies). The work of preparing International Standards is normally carried out through ISO technical committees. Each member body interested in a subject for which a technical committee has been established has the right to be represented on that committee. International organizations, governmental and non-governmental, in liaison with ISO, also take part in the work. ISO collaborates closely with the International Electrotechnical Commission (IEC) on all matters of electrotechnical standardization.

The procedures used to develop this document and those intended for its further maintenance are described in the ISO/IEC Directives, Part 1. In particular, the different approval criteria needed for the different types of ISO documents should be noted. This document was drafted in accordance with the editorial rules of the ISO/IEC Directives, Part 2 (see www.iso.org/directives).

Attention is drawn to the possibility that some of the elements of this document may be the subject of patent rights. ISO shall not be held responsible for identifying any or all such patent rights. Details of any patent rights identified during the development of the document will be in the Introduction and/or on the ISO list of patent declarations received (see www.iso.org/patents).

Any trade name used in this document is information given for the convenience of users and does not constitute an endorsement.

For an explanation of the voluntary nature of standards, the meaning of ISO specific terms and expressions related to conformity assessment, as well as information about ISO's adherence to the World Trade Organization (WTO) principles in the Technical Barriers to Trade (TBT) see www.iso.org/iso/foreword.html.

This document was prepared by Technical Committee ISO/TC 60, *Gears*, Subcommittee SC 2, *Gear capacity calculation*.

Any feedback or questions on this document should be directed to the user's national standards body. A complete listing of these bodies can be found at www.iso.org/members.html.

This first edition of ISO/TS 6336-22 cancels and replaces ISO/TR 15144-1:2014.

A list of all parts in the ISO 6336 series can be found on the ISO website. See also the Introduction for an overview.

Introduction

The ISO 6336 series consists of International Standards, Technical Specifications (TS) and Technical Reports (TR) under the general title *Calculation of load capacity of spur and helical gears* (see Table 1).

— International Standards contain calculation methods that are based on widely accepted practices and have been validated.

— TS contain calculation methods that are still subject to further development.

— TR contain data that is informative, such as example calculations.

The procedures specified in ISO 6336-1 to ISO 6336-19 cover fatigue analyses for gear rating. The procedures described in ISO 6336-20 to ISO 6336-29 are predominantly related to the tribological behaviour of the lubricated flank surface contact. ISO 6336-30 to ISO 6336-39 include example calculations. The ISO 6336 series allows the addition of new parts under appropriate numbers to reflect knowledge gained in the future.

Requesting standardized calculations according to ISO 6336 without referring to specific parts requires the use of only those parts that are currently designated as International Standards (see Table 1 for listing). When requesting further calculations, the relevant part or parts of ISO 6336 need to be specified. Use of a Technical Specification as acceptance criteria for a specific design needs to be agreed in advance between manufacturer and purchaser.

Table 1 — Overview of ISO 6336

Calculation of load capacity of spur and helical gears	International Standard	Technical Specification	Technical Report
Part 1: Basic principles, introduction and general influence factors	X		
Part 2: Calculation of surface durability (pitting)	X		
Part 3: Calculation of tooth bending strength	X		
Part 4: Calculation of tooth flank fracture load capacity		X	
Part 5: Strength and quality of materials	X		
Part 6: Calculation of service life under variable load	X		
Part 20: Calculation of scuffing load capacity (also applicable to bevel and hypoid gears) — Flash temperature method (Replaces: ISO/TR 13989-1)		X	
Part 21: Calculation of scuffing load capacity (also applicable to bevel and hypoid gears) — Integral temperature method (Replaces: ISO/TR 13989-2)		X	
Part 22: Calculation of micropitting load capacity (Replaces: ISO/TR 15144-1)		X	
Part 30: Calculation examples for the application of ISO 6336 parts 1, 2, 3, 5			X
Part 31: Calculation examples of micropitting load capacity (Replaces: ISO/TR 15144-2)			X
At the time of publication of this document, some of the parts listed here were under development. Consult the ISO website.			

This document provides principles for the calculation of the micropitting load capacity of cylindrical involute spur and helical gears with external teeth.

The basis for the calculation of the micropitting load capacity of a gear set is the model of the minimum operating specific lubricant film thickness in the contact zone. Many parameters can influence the occurrence of micropitting. These include surface topography, contact stress level, and lubricant chemistry. Whilst these parameters are known to affect the performance of micropitting for a gear set,

the subject area remains a topic of research and, as such, the science has not yet developed such that all aspects of these specific parameters are fully included in the calculation methods. Furthermore, the correct application of tip and root relief (involute modification) has been found to greatly influence micropitting; the suitable values should therefore be applied. Surface finish is another crucial parameter. At present, *R*a is used but other aspects such as *R*z or skewness have been observed to have significant effects which can be reflected in the finishing process applied.

Although the calculation of specific lubricant film thickness (which is also referred to in literature as "film thickness ratio" or "lambda ratio") does not provide a direct method for assessing micropitting load capacity, it can serve as an evaluation criterion when applied as part of a suitable comparative procedure based on known gear performance.

Calculation of load capacity of spur and helical gears —

Part 22:
Calculation of micropitting load capacity

1 Scope

This document describes a procedure for the calculation of the micropitting load capacity of cylindrical gears with external teeth. It has been developed on the basis of testing and observation of oil-lubricated gear transmissions with modules between 3 mm and 11 mm and pitch line velocities of 8 m/s to 60 m/s. However, the procedure is applicable to any gear pair where suitable reference data are available, providing the criteria specified below are satisfied.

The formulae specified are applicable for driving as well as for driven cylindrical gears with tooth profiles in line with the basic rack specified in ISO 53. They are also applicable for teeth conjugate to other basic racks where the virtual contact ratio ($\varepsilon_{\alpha n}$) is less than 2,5. The results are in good agreement with other methods for normal working pressure angles up to 25°, reference helix angles up to 25° and in cases where pitch line velocity is higher than 2 m/s.

This document is not applicable for the assessment of types of gear tooth surface damage other than micropitting.

2 Normative references

The following documents are referred to in the text in such a way that some or all of their content constitutes requirements of this document. For dated references, only the edition cited applies. For undated references, the latest edition of the referenced document (including any amendments) applies.

ISO 53, *Cylindrical gears for general and heavy engineering — Standard basic rack tooth profile*

ISO 1122-1, *Vocabulary of gear terms — Part 1: Definitions related to geometry*

ISO 1328-1, *Cylindrical gears — ISO system of flank tolerance classification — Part 1: Definitions and allowable values of deviations relevant to flanks of gear teeth*

ISO 6336-1, *Calculation of load capacity of spur and helical gears — Part 1: Basic principles, introduction and general influence factors*

ISO 6336-2, *Calculation of load capacity of spur and helical gears — Part 2: Calculation of surface durability (pitting)*

3 Terms, definitions, symbols and units

3.1 Terms and definitions

For the purposes of this document, the terms and definitions given in ISO 1122-1, ISO 6336-1 and ISO 6336-2 and the following apply.

ISO and IEC maintain terminological databases for use in standardization at the following addresses:

— ISO Online browsing platform: available at https://www.iso.org/obp

— IEC Electropedia: available at http://www.electropedia.org/

3.2 Symbols and units

The symbols used in this document are given in Table 2. The units of length metre, millimetre and micrometre are chosen in accordance with common practice. The conversions of the units are already included in the given formulae.

Table 2 — Symbols and units

Symbol	Description	Unit
a	centre distance	mm
A	ISO tolerance class according to ISO 1328-1	—
B_{M1}	thermal contact coefficient of pinion	N/(m·s^{0,5}·K)
B_{M2}	thermal contact coefficient of wheel	N/(m·s^{0,5}·K)
b	face width	mm
C	auxiliary constant	mm
C_{a1}	tip relief of pinion	µm
C_{a2}	tip relief of wheel	µm
C_{eff}	effective tip relief	µm
c_{M1}	specific heat capacity of pinion	J/(kg·K)
c_{M2}	specific heat capacity of wheel	J/(kg·K)
c'	maximum tooth stiffness per unit face width (single stiffness) of a tooth pair	N/(mm·µm)
$c_{\gamma\alpha}$	mean value of mesh stiffness per unit face width	N/(mm·µm)
d_{a1}	tip diameter of pinion	mm
d_{a2}	tip diameter of wheel	mm
d_{b1}	base diameter of pinion	mm
d_{b2}	base diameter of wheel	mm
d_{w1}	pitch diameter of pinion	mm
d_{w2}	pitch diameter of wheel	mm
d_{Y1}	Y-circle diameter of pinion	mm
d_{Y2}	Y-circle diameter of wheel	mm
E_r	reduced modulus of elasticity	N/mm^2
E_1	modulus of elasticity of pinion	N/mm^2
E_2	modulus of elasticity of wheel	N/mm^2
EAP	end of active profile (for driving pinion: contact point E, for driving wheel: contact point A)	—
F_{bt}	nominal transverse load in plane of action (base tangent plane)	N
F_t	(nominal) transverse tangential load at reference cylinder per mesh	N
G_M	material parameter	—
g_Y	parameter on the path of contact (distance of point Y from point A)	mm
g_α	length of path of contact	mm
H_v	load losses factor	—
h_Y	local lubricant film thickness	µm
K_A	application factor	—
$K_{B\gamma}$	helical load factor	—
$K_{H\alpha}$	transverse load factor	—
$K_{H\beta}$	face load factor	—
K_v	dynamic factor	—
K_γ	mesh load factor	—

Table 2 *(continued)*

Symbol	Description	Unit
n_1	rotation speed of pinion	min^{-1}
P	transmitted power	kW
p_{et}	transverse base pitch on the path of contact	mm
$p_{dyn,Y}$	local Hertzian contact stress including the load factors K	N/mm^2
$p_{H,Y}$	local nominal Hertzian contact stress	N/mm^2
Ra	effective arithmetic mean roughness value	µm
Ra_1	arithmetic mean roughness value of pinion	µm
Ra_2	arithmetic mean roughness value of wheel	µm
$S_{GF,Y}$	local sliding parameter	—
S_λ	safety factor against micropitting	—
$S_{\lambda,min}$	minimum required safety factor against micropitting	—
SAP	start of active profile (for driving pinion: contact point A, for driving wheel: contact point E)	—
T_1	nominal torque at the pinion	Nm
U_Y	local velocity parameter	—
u	gear ratio	—
$v_{g,Y}$	local sliding velocity	m/s
VI	viscosity index	—
$v_{r1,Y}$	local tangential velocity on pinion	m/s
$v_{r2,Y}$	local tangential velocity on wheel	m/s
$v_{\Sigma,C}$	sum of tangential velocities at pitch point	m/s
$v_{\Sigma,Y}$	sum of tangential velocities at point Y	m/s
W_W	material factor	—
W_Y	local load parameter	—
$X_{but,Y}$	local buttressing factor	—
X_{Ca}	tip relief factor	—
X_L	lubricant factor	—
X_R	roughness factor	—
X_S	lubrication factor	—
X_Y	local load sharing factor	—
Z_E	elasticity factor	$(N/mm^2)^{0,5}$
z_1	number of teeth of pinion	—
z_2	number of teeth of wheel	—
α_t	transverse pressure angle	°
α_{wt}	pressure angle at the pitch cylinder	°
$\alpha_{\theta B,Y}$	pressure-viscosity coefficient at local contact temperature	m^2/N
$\alpha_{\theta M}$	pressure-viscosity coefficient at bulk temperature	m^2/N
α_{38}	pressure-viscosity coefficient at 38 °C	m^2/N
β_b	base helix angle	°
ε_{max}	maximum addendum contact ratio	—
ε_α	transverse contact ratio	—
$\varepsilon_{\alpha n}$	virtual contact ratio, transverse contact ratio of a virtual spur gear	—
ε_β	overlap ratio	—
ε_γ	total contact ratio	—

Table 2 *(continued)*

Symbol	Description	Unit
ε_1	addendum contact ratio of the pinion	—
ε_2	addendum contact ratio of the wheel	—
$\eta_{\theta B,Y}$	dynamic viscosity at local contact temperature	N·s/m^2
$\eta_{\theta M}$	dynamic viscosity at bulk temperature	N·s/m^2
$\eta_{\theta oil}$	dynamic viscosity at oil inlet/sump temperature	N·s/m^2
η_{38}	dynamic viscosity at 38 °C	N·s/m^2
$\theta_{B,Y}$	local contact temperature	°C
$\theta_{fl,Y}$	local flash temperature	°C
θ_M	bulk temperature	°C
θ_{oil}	oil inlet/sump temperature	°C
$\lambda_{GF,min}$	minimum specific lubricant film thickness in the contact area	—
$\lambda_{GF,Y}$	local specific lubricant film thickness	—
λ_{GFP}	permissible specific lubricant film thickness	—
λ_{GFT}	limiting specific lubricant film thickness of the test gears	—
λ_{M1}	specific heat conductivity of pinion	W/(m·K)
λ_{M2}	specific heat conductivity of wheel	W/(m·K)
μ_m	mean coefficient of friction	—
$\nu_{\theta B,Y}$	kinematic viscosity at local contact temperature	mm^2/s
$\nu_{\theta M}$	kinematic viscosity at bulk temperature	mm^2/s
ν_1	Poisson's ratio of pinion	—
ν_2	Poisson's ratio of wheel	—
ν_{100}	kinematic viscosity at 100 °C	mm^2/s
ν_{40}	kinematic viscosity at 40 °C	mm^2/s
ρ_{M1}	density of pinion	kg/m^3
ρ_{M2}	density of wheel	kg/m^3
$\rho_{n,C}$	normal radius of relative curvature at pitch diameter	mm
$\rho_{n,Y}$	normal radius of relative curvature at point Y	mm
$\rho_{t,Y}$	transverse radius of relative curvature at point Y	mm
$\rho_{t1,Y}$	transverse radius of curvature of pinion at point Y	mm
$\rho_{t2,Y}$	transverse radius of curvature of wheel at point Y	mm
$\rho_{\theta B,Y}$	density of lubricant at local contact temperature	kg/m^3
$\rho_{\theta M}$	density of lubricant at bulk temperature	kg/m^3
ρ_{15}	density of lubricant at 15 °C	kg/m^3
Subscripts to symbols		
Y	parameter for any contact point Y in the contact area for Method A and on the path of contact for Method B; (all parameters subscript Y have to be calculated with local values)	

4 Micropitting

Micropitting is a phenomenon that occurs in Hertzian type of rolling and sliding contact that operates in mixed elastohydrodynamic or boundary lubrication regimes. Micropitting is influenced by operating conditions such as load, speed, sliding, temperature, surface topography, specific lubricant film thickness and chemical composition of the lubricant. Micropitting is more commonly observed on materials with a high surface hardness.

Micropitting is the generation of numerous surface cracks. The cracks grow at a shallow angle to the surface forming micropits. The micropits are small relative to the size of the contact zone, typically of the order 10 µm to 20 µm deep. The micropits can coalesce to produce a continuous fractured surface which appears as a dull, matte surface during unmagnified visual inspection.

Micropitting is the preferred name for this phenomenon, but it has also been referred to as grey staining, grey flecking, frosting and peeling, see ISO 10825.

Micropitting can arrest. However, if micropitting continues to progress, it can result in reduced gear tooth accuracy, increased dynamic loads and noise. If it does not arrest and continues to propagate it can develop into macropitting and other modes of gear failure.

5 Basic formulae

5.1 General

The calculation of micropitting load capacity is based on the local specific lubricant film thickness, $\lambda_{GF,Y}$, in the contact area and the permissible specific lubricant film thickness, λ_{GFP}[11]. It is assumed that micropitting can occur, when the minimum specific lubricant film thickness, $\lambda_{GF,min}$, is lower than a corresponding critical value, λ_{GFP}. Both values, $\lambda_{GF,min}$ and λ_{GFP}, shall be calculated separately for pinion and wheel in the contact area. It needs to be recognized that the determination of the minimum specific lubricant film thickness and the permissible specific lubricant film thickness shall be based on the operating parameters.

The formulae specified are applicable for driving as well as driven cylindrical gears with tooth profiles in accordance with the basic rack specified in ISO 53. They are also applicable for teeth conjugate to other basic racks where the virtual contact ratio ($\varepsilon_{\alpha n}$) is less than 2,5.

The bulk temperature is established by the thermal balance of the gear unit. There are several sources of heat in a gear unit of which the most important are tooth and bearing friction. Other sources of heat such as seals and oilflow contribute to some extent. At pitch line velocities in excess of 80 m/s, heat from the churning of oil in the mesh and windage losses can become significant and should be taken into consideration (see Method A). The heat is transferred to the environment via the housing walls by conduction, convection and radiation and for spray lubrication conditions through the oil into an external heat exchanger.

With decreasing pitch line velocities, the lubricant film thickness, h, and consequently the safety factor against micropitting, S_λ, are decreasing. In low speed applications, wear can become the dominant mechanism. This has been observed in experimental investigations with lubricant film thicknesses at the pitch point $h_C \leq 0{,}1$ µm. For such applications, experimental investigations according to Method A or Method B under representative (test) conditions should be carried out for lubricant film thicknesses similar to those at operating conditions in order to verify if micropitting still is the main mechanism.

The micropitting load capacity can be determined by comparing the minimum specific lubricant film thickness with the corresponding limiting value derived from gears in service or from specific gear testing. This comparison is expressed by the safety factor, S_λ, which shall be equal to or higher than a minimum safety factor against micropitting, $S_{\lambda,min}$.

Micropitting mainly occurs in areas of negative specific sliding. Negative specific sliding is to be found along the path of contact between point A and C on the driving gear and between point C and E on the driven gear. Considering the influences of lubricant, surface roughness, geometry of the gears and operating conditions the specific lubricant film thickness, $\lambda_{GF,Y}$, can be calculated for every point in the field of contact.

5.2 Safety factor against micropitting, S_λ

To account for the micropitting load capacity the safety factor, S_λ, according to Formula (1) is defined:

$$S_\lambda = \frac{\lambda_{GF,min}}{\lambda_{GFP}} \geq S_{\lambda,min} \quad (1)$$

where

$\lambda_{GF,min} = \min(\lambda_{GF,Y})$ is the minimum specific lubricant film thickness in the contact area;

$\lambda_{GF,Y}$ is the local specific lubricant film thickness (see 5.3);

λ_{GFP} is the permissible specific lubricant film thickness (see 5.4);

$S_{\lambda,min}$ is the minimum required safety factor (see 5.5).

The minimum specific lubricant film thickness is determined from all calculated local values of the specific lubricant film thickness, $\lambda_{GF,Y}$, obtained by Formula (2).

5.3 Local specific lubricant film thickness, $\lambda_{GF,Y}$

For the determination of the safety factor, S_λ, the local lubricant film thickness, h_Y, according to Dowson/Higginson[5] in the field of contact has to be known and compared with the effective surface roughness:

$$\lambda_{GF,Y} = \frac{h_Y}{Ra} \quad (2)$$

where

$$Ra = 0{,}5 \cdot (Ra_1 + Ra_2) \quad (3)$$

$$h_Y = 1\,600 \cdot \rho_{n,Y} \cdot G_M^{0,6} \cdot U_Y^{0,7} \cdot W_Y^{-0,13} \cdot S_{GF,Y}^{0,22} \quad (4)$$

where

Ra is the effective arithmetic mean roughness value;

Ra_1 is the arithmetic mean roughness value of pinion (see ISO 6336-2);

Ra_2 is the arithmetic mean roughness value of wheel (see ISO 6336-2);

h_Y is the local lubricant film thickness;

$\rho_{n,Y}$ is the normal radius of relative curvature at point Y (see Clause 10);

G_M is the material parameter (see Clause 6);

U_Y is the local velocity parameter (see Clause 7);

W_Y is the local load parameter (see Clause 8);

$S_{GF,Y}$ is the local sliding parameter (see Clause 9).

Formula (4) should be calculated in the case of Method B at the seven local points (Y) defined in 5.3 b) using the values for $\rho_{n,Y}$, U_Y, W_Y and $S_{GF,Y}$ that exists at each point Y. The minimum of the seven h_Y ($\lambda_{GF,Y}$) values shall be used in Formula (1).

Example calculations are presented in ISO/TR 6336-31.

a) **Method A**

The local specific lubricant film thickness can be determined in the complete contact area by any appropriate gear computing program. In order to determine the local specific lubricant film thickness, the load distribution, the influence of normal and sliding velocity with changes of meshing phase and the actual service conditions shall be taken into consideration.

b) **Method B**

This method involves the assumption that the determinant local specific lubricant film thickness occurs on the tooth flank in the area of negative sliding. For simplification, the calculation of the local specific lubricant film thickness is limited to certain points on the path of contact. For this purpose, the following points are surveyed:

— the lower point A and upper point E on the path of contact;

— the lower point B and upper point D of single pair tooth contact;

— the midway point AB between A and B;

— the midway point DE between D and E; and

— the pitch point C.

Furthermore, for the calculation, two cases are differentiated:

— case 1: no profile modification;

— case 2: adequate profile modification according to manufacturer's experience.

In case of profile modifications lower than adequate profile modifications, case 1 shall be used. In case of too high profile modifications, it is recommended to use Method A.

NOTE If the calculated film thickness at pitch point $h_C \leq 0{,}1$ µm, refer to the scope for discussion of the potential risk of wear.

5.4 Permissible specific lubricant film thickness, λ_{GFP}

For the determination of the permissible specific lubricant film thickness, λ_{GFP}, different procedures are applicable.

a) **Method A**

For Method A, experimental investigations or service experience relating to micropitting on real gears are used.

Running real gears under conditions where micropitting just occurs the minimum specific lubricant film thickness can be calculated according to 5.3 a). This value is equivalent to the limiting specific lubricant film thickness which is used to calculate the micropitting load capacity.

Such experimental investigations can be performed on gears having the same design as the actual gear pair. In this case, the gear manufacturing, gear accuracy, operating conditions, lubricant and operating temperature shall be appropriate for the actual gear pair.

The cost required for this method is in general only justifiable for the development of new products as well as for gear pairs where failure would have serious consequences.

Otherwise, the permissible specific lubricant film thickness, λ_{GFP}, can be derived from consideration of dimensions, service conditions and performance of carefully monitored reference gears operated with the respective lubricant. The more closely the dimensions and service conditions of the actual

gears resemble those of the reference gears, the more effective will be the application of such values for the purpose of design ratings or calculation checks.

b) **Method B**

The method adapted is validated by carrying out careful comparative studies of well-documented histories of a number of test gears applicable to the type, quality and manufacture of gearing under consideration. The permissible specific lubricant film thickness, λ_{GFP}, is calculated from the critical specific lubricant film thickness, λ_{GFT}, which is the result of any standardized test method applicable to evaluate the micropitting load capacity of lubricants or materials by means of defined test gears operated under specified test conditions. λ_{GFT} is a function of the temperature, oil viscosity, base oil and additive chemistry and can be calculated according to Formula (2) in the contact point of the defined test gears where the minimum specific lubricant film thickness is to be found and for the test conditions where the failure limit concerning micropitting in the standardized test procedure has been reached.

The test gears as well as the test conditions (for example the test temperature) shall be appropriate for the real gears in consideration.

Any standardized test can be used to determine the data. Where a specific test procedure is not available or required, a number of internationally available standardized test methods for the evaluation of micropitting performance of gears, lubricants and materials are currently available. Some widely used test procedures are the FVA-FZG-micropitting test[7], Flender micropitting test[12], BGA-DU micropitting test[2] and the micropitting test according to [3]. Annex A provides some generalized test data (for reference only) that have been produced using the test procedure according to FVA-Information Sheet 54/7[7] where a value for λ_{GFP} can be calculated for a generalized reference allowable using Formula A.1.

Micropitting load capacity is significantly influenced by additives, often more than by the viscosity. As the effectiveness of additives depends significantly on temperature, it is recommended to test the oil at the temperature used in the application, i.e. in the range of approximately ±15 K. If the difference is higher, a specific test should be performed or an additional safety margin considered and agreed between customer and manufacturer. Normally, micropitting tests are executed at specific oil injection temperatures. The data from oil providers shall contain the failure load stage SKS and the test temperature.

The permissible specific lubricant film thickness, λ_{GFP}, should be determined based on experimental investigations or service experience. If no such data or experiences are available, some generalized data (for reference only) are provided in Annex B.

5.5 Recommendation for the minimum safety factor against micropitting, $S_{\lambda,min}$

For a given application, adequate micropitting load capacity is demonstrated by the computed value of S_λ and being greater than or equal to the value $S_{\lambda,min}$, respectively.

Micropitting can stop after a period of running or it can progress to macropitting and failure. Although there are criteria to define micropitting failure for lubricant testing, there are no universally applied criteria available to define when micropitting is considered to be damaging.

Certain minimum values for the safety factor, which is defined in this document as the ratio of calculated minimum specific film thickness to permissible specific film thickness [see Formula (1)], shall be determined.

An appropriate probability of failure and corresponding safety factor shall be carefully chosen to meet the required reliability at a justifiable cost. Depending on the reliability of the assumptions on which the calculations are based (for example, load assumptions) and according to the reliability requirements (consequences of occurrence), a corresponding safety factor is selected.

Where gears are produced according to a specification or a request for proposal (quotation), in which the gear supplier is to provide gears or assembled gear drives having specified calculated capacities

(ratings) in accordance with this document, the value of the safety factor for micropitting is to be agreed between the parties.

In addition to the general requirements mentioned and the special requirements for specific lubricant film thickness, the safety factor shall be chosen after careful consideration of the following influences.

— If the application is critical, has strict noise requirements, or is sensitive to wear particles in the lube, it may be tolerated to have no micropitting. The profile and lead modifications of the gear teeth should be designed using 3D contact analysis. The flank roughness should be controlled such that the sum of the contact asperities is well below the oil film thickness. A higher safety factor corresponds to a conservative design.

— If the performance of the gears can be accurately appraised through testing of the actual unit under actual load conditions, a lower safety factor and more economical manufacturing procedures may be permissible.

— If there are variations in manufacturing processes, especially variations in gear geometry and surface texture due to manufacturing tolerances, variations in alignment, or variations in material due to process variations in chemistry, cleanliness, and microstructure (material quality and heat treatment), a larger safety factor may be required.

— If there is uncertainty in the gear drive application because the loads or the response of the system to vibration are estimated rather than measured, a larger safety factor should be used.

— If there are variations in the lubrication and maintenance of the gear drive over the service life of the gears, a larger safety factor should be used.

— In general industrial service, some degree of micropitting may be tolerated so long as it does not progress rapidly. If micropitting is observed, it should be recorded and the gearing regularly checked to determine whether the pattern is growing. The lubricant may also be changed more frequently, filtered to remove wear particles, or a different lubricant with higher micropitting resistance may be used. In this case, a lower safety factor may be acceptable and micropitting by itself may not be considered a failure.

6 Material parameter, G_M

6.1 General

The material parameter, G_M, accounts for the influence of the reduced modulus of elasticity, E_r, and the pressure-viscosity coefficient of the lubricant at bulk temperature, $\alpha_{\theta M}$:

$$G_M = 10^6 \cdot \alpha_{\theta M} \cdot E_r \tag{5}$$

where

E_r is the reduced modulus of elasticity (see 6.2);

$\alpha_{\theta M}$ is the pressure-viscosity coefficient at bulk temperature (see 6.3).

6.2 Reduced modulus of elasticity, E_r

For mating gears of different material and modulus of elasticity, E_1 and E_2, the reduced modulus of elasticity, E_r, can be determined by Formula (6). For mating gears of the same material $E = E_1 = E_2$, Formula (7) can be used.

$$E_r = 2 \cdot \left(\frac{1-\nu_1^2}{E_1} + \frac{1-\nu_2^2}{E_2} \right)^{-1} \tag{6}$$

$$E_r = \frac{E}{1-\nu^2} \quad \text{for } E_1 = E_2 = E \text{ and } \nu_1 = \nu_2 = \nu \tag{7}$$

where

E_1 is the modulus of elasticity of pinion (for steel: E = 206 000 N/mm^2);

E_2 is the modulus of elasticity of wheel (for steel: E = 206 000 N/mm^2);

ν_1 is the Poisson's ratio of pinion (for steel: ν = 0,3);

ν_2 is the Poisson's ratio of wheel (for steel: ν = 0,3).

6.3 Pressure viscocity coefficient at bulk temperature, $\alpha_{\theta M}$

If the data for the pressure-viscosity coefficient at bulk temperature, $\alpha_{\theta M}$, for the specific lubricant is not available, it can be approximated using Formula (8) (see [8]):

$$\alpha_{\theta M} = \alpha_{38} \cdot \left[1 + 516 \cdot \left(\frac{1}{\theta_M + 273} - \frac{1}{311} \right) \right] \tag{8}$$

where

α_{38} is the pressure-viscosity coefficient of the lubricant at 38 °C;

θ_M is the bulk temperature (see Clause 14).

If no values for α_{38} are available, they can be approximated using Formulae (9) to (11) [1]:

$$\alpha_{38} = 2{,}657 \cdot 10^{-8} \cdot \eta_{38}^{0{,}1348} \quad \text{for mineral oil} \tag{9}$$

$$\alpha_{38} = 1{,}466 \cdot 10^{-8} \cdot \eta_{38}^{0{,}0507} \quad \text{for PAO-based synthetic non-VI improved oil} \tag{10}$$

$$\alpha_{38} = 1{,}392 \cdot 10^{-8} \cdot \eta_{38}^{0{,}1572} \quad \text{for PAG-based synthetic oil} \tag{11}$$

where η_{38} is the dynamic viscosity of the lubricant at 38 °C.

7 Local velocity parameter, U_Y

7.1 General

The local velocity parameter, U_Y, calculated with Formula (12), describes the proportional increase of the specific lubricant film thickness with increasing dynamic viscosity, $\eta_{\theta M}$, of the lubricant at bulk temperature and sum of the tangential velocities, $v_{\Sigma,Y}$:

$$U_Y = \eta_{\theta M} \cdot \frac{v_{\Sigma,Y}}{2\,000 \cdot E_r \cdot \rho_{n,Y}} \tag{12}$$

where

$\eta_{\theta M}$ is the dynamic viscosity of the lubricant at bulk temperature (see 7.3);

$v_{\Sigma,Y}$ is the sum of the tangential velocities at point Y (see 7.2);

E_r is the reduced modulus of elasticity (see 6.2);

$\rho_{n,Y}$ is the local normal radius of relative curvature at point Y (see Clause 10).

7.2 Sum of tangential velocities, $v_{\Sigma,Y}$

The sum of the tangential velocities at a mesh point Y is calculated according to Formulae (13) to (15). The velocity for pinion, $v_{r1,Y}$, and wheel, $v_{r2,Y}$, in a certain contact point Y on the tooth flank depends on the diameter at pinion, d_{Y1}, and the diameter at wheel, d_{Y2}, of point Y.

$$v_{\Sigma,Y} = v_{r1,Y} + v_{r2,Y} \tag{13}$$

where

$$v_{r1,Y} = 2 \cdot \pi \cdot \frac{n_1}{60} \cdot \frac{d_{w1}}{2\,000} \cdot \sin\alpha_{wt} \cdot \sqrt{\frac{d_{Y1}^2 - d_{b1}^2}{d_{w1}^2 - d_{b1}^2}} \tag{14}$$

$$v_{r2,Y} = 2 \cdot \pi \cdot \frac{n_1}{u \cdot 60} \cdot \frac{d_{w2}}{2\,000} \cdot \sin\alpha_{wt} \cdot \sqrt{\frac{d_{Y2}^2 - d_{b2}^2}{d_{w2}^2 - d_{b2}^2}} \tag{15}$$

$v_{r1,Y}$ is the tangential velocity on pinion (see Figure 1);

$v_{r2,Y}$ is the tangential velocity on wheel (see Figure 1);

d_{b1} is the base diameter of pinion;

d_{b2} is the base diameter of wheel;

d_{w1} is the pitch diameter of pinion;

d_{w2} is the pitch diameter of wheel;

d_{Y1} is the Y-circle diameter of pinion (see Figure 1 and Clause 10);

d_{Y2} is the Y-circle diameter of wheel (see Figure 1 and Clause 10);

n_1 is the rotation speed of pinion;

$u = z_2/z_1$ is the gear ratio;

α_{wt} is the pressure angle at the pitch cylinder.

7.3 Dynamic viscosity at bulk temperature, $\eta_{\theta M}$

7.3.1 General

The dynamic viscosity at bulk temperature, $\eta_{\theta M}$, can be calculated according to Formula (16):

$$\eta_{\theta M} = 10^{-6} \cdot \nu_{\theta M} \cdot \rho_{\theta M} \tag{16}$$

where

$\nu_{\theta M}$ is the kinematic viscosity of the lubricant at bulk temperature (see 7.3.2);

$\rho_{\theta M}$ is the density of the lubricant at bulk temperature (see 7.3.3).

7.3.2 Kinematic viscosity at bulk temperature, $\nu_{\theta M}$

The kinematic viscosity at bulk temperature, $\nu_{\theta M}$, can be calculated from the kinematic viscosity at 40 °C, ν_{40}, and the kinematic viscosity at 100 °C, ν_{100}, on the basis of Formulae (17) to (19). Extrapolation for temperature higher than 140 °C should be confirmed by measurement.

$$\log\left[\log\left(\nu_{\theta M} + 0{,}7\right)\right] = A \cdot \log\left(\theta_M + 273\right) + B \tag{17}$$

where

$$A = \frac{\log\left[\log\left(\nu_{40} + 0{,}7\right) / \log\left(\nu_{100} + 0{,}7\right)\right]}{\log\left(313/373\right)} \tag{18}$$

$$B = \log\left[\log\left(\nu_{40} + 0{,}7\right)\right] - A \cdot \log\left(313\right) \tag{19}$$

where

θ_M is the bulk temperature (see Clause 14);

ν_{40} is the kinematic viscosity of the lubricant at 40 °C;

ν_{100} is the kinematic viscosity of the lubricant at 100 °C.

7.3.3 Density of the lubricant at bulk temperature, $\rho_{\theta M}$

If the density of the lubricant at bulk temperature, $\rho_{\theta M}$, is not available, it can be approximated based on the density of the lubricant at 15 °C according to Formula (20):

$$\rho_{\theta M} = \rho_{15} \cdot \left[1 - 0{,}7 \cdot \frac{\left(\theta_M + 273\right) - 288}{\rho_{15}}\right] \tag{20}$$

where

ρ_{15} is the density of the lubricant at 15 °C according to the lubricant data sheet;

θ_M is the bulk temperature (see Clause 14).

If no data for ρ_{15} is available, then Formula (21) can be used for approximation of mineral oils[10]:

$$\rho_{15} = 43{,}37 \cdot \log \nu_{40} + 805{,}5 \tag{21}$$

where ν_{40} is the kinematic viscosity of the lubricant at 40 °C.

8 Local load parameter, W_Y

8.1 General

The local load parameter, W_Y, can be determined using the local Hertzian contact stress, $p_{dyn,Y}$, and the reduced modulus of elasticity, E_r, as shown in Formula (22):

$$W_Y = \frac{2 \cdot \pi \cdot p_{dyn,Y}^2}{E_r^2} \tag{22}$$

where

$p_{dyn,Y}$ is the local Hertzian contact stress according to Method A (see 8.2) or according to Method B (see 8.3);

E_r is the reduced modulus of elasticity (see 6.2).

8.2 Local Hertzian contact stress, $p_{dyn,Y,A}$, according to Method A

The local Hertzian contact stress, $p_{dyn,Y,A}$, according to Method A should be determined by means of a 3D mesh contact and load distribution analysis procedure. The local nominal Hertzian contact stress determined from the elastic mesh contact model $p_{H,Y,A}$ is applied to Formula (23) to obtain the local Hertzian contact stress, $p_{dyn,Y,A}$:

$$p_{dyn,Y,A} = p_{H,Y,A} \cdot \sqrt{K_A \cdot K_v} \tag{23}$$

where

$p_{H,Y,A}$ is the local nominal Hertzian contact stress, calculated with a 3D load distribution program;

K_A is the application factor (according to ISO 6336-1);

K_v is the dynamic factor (according to ISO 6336-1).

NOTE Where either K_A or K_v influences are already considered in the 3D elastic mesh contact model, either K_A or K_v (or both) should be set at 1,0 in Formula (23).

8.3 Local Hertzian contact stress, $p_{dyn,Y,B}$, according to Method B

8.3.1 General

The local Hertzian contact stress, $p_{dyn,Y,B}$, according to Method B is calculated according to Formula (24). The required nominal Hertzian contact stress, $p_{H,Y,B}$, is obtained by Formulae (25) and (26), see 8.3.2.

$$p_{dyn,Y,B} = p_{H,Y,B} \cdot \sqrt{K_A \cdot K_\gamma \cdot K_v \cdot K_{H\alpha} \cdot K_{H\beta}} \tag{24}$$

where

$p_{H,Y,B}$ is the local nominal Hertzian contact stress (see 8.3.2);

K_A is the application factor (according to ISO 6336-1);

K_γ is the mesh load factor (according to ISO 6336-1);

K_v is the dynamic factor (according to ISO 6336-1);

$K_{H\alpha}$ is the transverse load factor (according to ISO 6336-1). Profile modifications are considered in the factor X_Y, see Clause 11.

$K_{H\beta}$ is the face load factor (according to ISO 6336-1). Lead modifications are considered in this factor.

NOTE Gears with a transverse contact ratio $\varepsilon_\alpha > 2$ can only be calculated according to Method A.

8.3.2 Local nominal Hertzian contact stress, $p_{H,Y,B}$

The local nominal Hertzian contact stress, $p_{H,Y,B}$, is used to determine the local Hertzian contact stress, $p_{dyn,Y,B}$, (see 8.2). To take the influence of different profile modifications into account the load sharing factor, X_Y, is introduced. For the calculation of the local nominal Hertzian contact stress, the local nominal radius of relative curvature is used.

$$p_{H,Y,B} = Z_E \cdot \sqrt{\frac{F_t \cdot X_Y}{b \cdot \rho_{n,Y} \cdot \cos\alpha_t}} \tag{25}$$

where

$$Z_E = \sqrt{\frac{E_r}{2 \cdot \pi}} \tag{26}$$

Z_E is the elasticity factor (according to ISO 6336-2);

b is the face width;

F_t is the transverse tangential load at reference cylinder;

X_Y is the load sharing factor (see Clause 11);

E_r is the reduced modulus of elasticity (see 6.2);

α_t is the transverse pressure angle;

β_b is the base helix angle;

$\rho_{n,Y}$ is the local normal radius of relative curvature (see Clause 10).

9 Local sliding parameter, $S_{GF,Y}$

9.1 General

The local sliding parameter, $S_{GF,Y}$ [see Formula (27)], accounts for the influence of local sliding on the local temperature. This temperature influences both the local pressure-viscosity coefficient and the local dynamic viscosity and hence the local lubricant film thickness[6]. The local contact temperature, $\theta_{B,Y}$, is the sum of the local flash temperature, $\theta_{fl,Y}$, and the bulk temperature, θ_M.

$$S_{GF,Y} = \frac{\alpha_{\theta B,Y} \cdot \eta_{\theta B,Y}}{\alpha_{\theta M} \cdot \eta_{\theta M}} \tag{27}$$

where

$\alpha_{\theta B,Y}$ is the pressure-viscosity coefficient at local contact temperature (see 9.2);

$\eta_{\theta B,Y}$ is the dynamic viscosity at local contact temperature (see 9.3);

$\alpha_{\theta M}$ is the pressure-viscosity coefficient at bulk temperature (see 6.3);

$\eta_{\theta M}$ is the dynamic viscosity at bulk temperature (see 7.3).

9.2 Pressure viscosity coefficient at local contact temperature, $\alpha_{\theta B,Y}$

If the data for the pressure-viscosity coefficient at local contact temperature, $\alpha_{\theta B,Y}$, for the specific lubricant is not available, it can be approximated by Formula (28) (see [8]):

$$\alpha_{\theta B,Y} = \alpha_{38} \cdot \left[1 + 516 \cdot \left(\frac{1}{\theta_{B,Y} + 273} - \frac{1}{311} \right) \right] \tag{28}$$

where

α_{38} is the pressure-viscosity coefficient of the lubricant at 38 °C (see also 6.3);

$\theta_{B,Y}$ is the local contact temperature (see Clause 12).

9.3 Dynamic viscosity at local contact temperature, $\eta_{\theta B,Y}$

9.3.1 General

The dynamic viscosity at local contact temperature, $\eta_{\theta B,Y}$, is determined by Formula (29):

$$\eta_{\theta B,Y} = 10^{-6} \cdot \nu_{\theta B,Y} \cdot \rho_{\theta B,Y} \tag{29}$$

where

$\nu_{\theta B,Y}$ is the kinematic viscosity at local contact temperature (see 9.3.2);

$\rho_{\theta B,Y}$ is the density of the lubricant at local contact temperature (see 9.3.3).

9.3.2 Kinematic viscosity at local contact temperature, $\nu_{\theta B,Y}$

The kinematic viscosity at local contact temperature, $\nu_{\theta B,Y}$, can be calculated from the kinematic viscosity at 40 °C, ν_{40}, and the kinematic viscosity at 100 °C, ν_{100}, on the basis of Formula (30). Extrapolation for temperature higher than 140 °C should be confirmed by measurement.

$$\log\left[\log\left(\nu_{\theta B,Y}+0{,}7\right)\right]=A\cdot\log\left(\theta_{B,Y}+273\right)+B \tag{30}$$

where

A is determined according to Formula (18);

B is determined according to Formula (19);

$\theta_{B,Y}$ is the local contact temperature (see Clause 12);

ν_{40} is the kinematic viscosity of the lubricant at 40 °C;

ν_{100} is the kinematic viscosity of the lubricant at 100 °C.

9.3.3 Density of the lubricant at local contact temperature, $\rho_{\theta B,Y}$

If the density of the lubricant at local contact temperature, $\rho_{\theta B,Y}$, is not available, it can be approximated based on the density of the lubricant at 15 °C according to Formula (31):

$$\rho_{\theta B,Y}=\rho_{15}\cdot\left[1-0{,}7\cdot\frac{\left(\theta_{B,Y}+273\right)-288}{\rho_{15}}\right] \tag{31}$$

where

ρ_{15} is the density of the lubricant at 15 °C according to the lubricant data sheet (see also 7.3.3);

$\theta_{B,Y}$ is the local contact temperature (see Clause 12).

10 Definition of contact point Y on the path of contact

Contact point Y is located between the SAP (for driving pinion: contact point A, for driving wheel: contact point E) and EAP (for driving pinion: contact point E, for driving wheel: contact point A) on the path of contact according to Figure 1. It describes the actual contact point between pinion and wheel in a certain meshing position, g_Y.

According to 5.3, Method B, the calculation shall be done for the following contact points, using Formulae (32) to (38):

Y =

A $g_Y=g_A=0\ \text{mm}$ the lower point on the path of contact (32)

AB $g_Y=g_{AB}=\left(g_\alpha-p_{et}\right)/2$ the midway point between A and B (33)

B $g_Y=g_B=g_\alpha-p_{et}$ the lower point of single pair tooth contact (34)

C $g_Y=g_C=\frac{d_{b1}}{2}\cdot\tan\alpha_{wt}-\sqrt{\frac{d_{a1}^2}{4}-\frac{d_{b1}^2}{4}}+g_\alpha$ the pitch point (35)

D $g_Y = g_D = p_{et}$ the upper point of single pair tooth contact (36)

DE $g_Y = g_{DE} = (g_\alpha - p_{et})/2 + p_{et}$ the midway point between D and E (37)

E $g_Y = g_E = g_\alpha$ the upper point on the contact path (38)

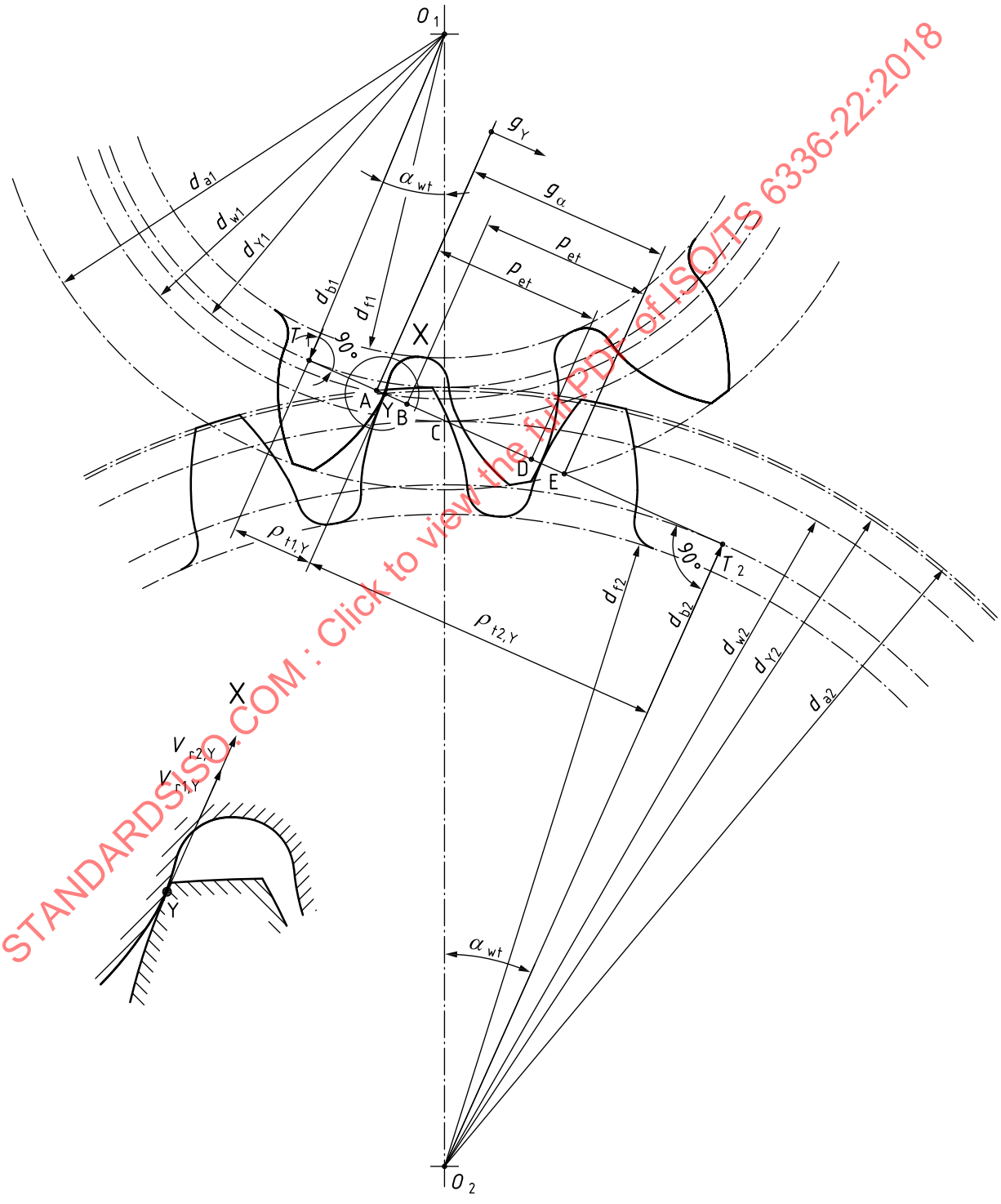

Figure 1 — Definition of contact point Y on the line of action

The Y-circle diameter of pinion, d_{Y1}, and wheel, d_{Y2}, are dependent on the location contact point Y on the path of contact, g_Y, and can be calculated according to Formulae (39) and (40):

$$d_{Y1} = 2 \cdot \sqrt{\frac{d_{b1}^2}{4} + \left(\sqrt{\frac{d_{a1}^2}{4} - \frac{d_{b1}^2}{4}} - g_\alpha + g_Y \right)^2} \tag{39}$$

$$d_{Y2} = 2 \cdot \sqrt{\frac{d_{b2}^2}{4} + \left(\sqrt{\frac{d_{a2}^2}{4} - \frac{d_{b2}^2}{4}} - g_Y \right)^2} \tag{40}$$

where

d_{a1} is the tip diameter of pinion (see Figure 1);

d_{a2} is the tip diameter of wheel (see Figure 1);

d_{b1} is the base diameter of pinion (see Figure 1);

d_{b2} is the base diameter of wheel (see Figure 1);

g_Y is the parameter on the path of contact (see Figure 1);

g_α is the length of path of contact (see Figure 1).

The transverse radius of relative curvature, $\rho_{t,Y}$, can be determined according to Formulae (41) and (42):

$$\rho_{t,Y} = \frac{\rho_{t1,Y} \cdot \rho_{t2,Y}}{\rho_{t1,Y} + \rho_{t2,Y}} \tag{41}$$

where

$$\rho_{t1,2,Y} = \sqrt{\frac{d_{Y1,2}^2 - d_{b1,2}^2}{4}} \tag{42}$$

$\rho_{t1,2,Y}$ is the transverse radius of curvature of pinion/ wheel at point Y (see Figure 1);

$d_{b1,2}$ is the base diameter of pinion/ wheel (see Figure 1);

$d_{Y1,2}$ is the Y-circle diameter of pinion/ wheel (see above and Figure 1).

The normal radius of relative curvature, $\rho_{n,Y}$, can be calculated according to Formula (43):

$$\rho_{n,Y} = \frac{\rho_{t,Y}}{\cos\beta_b} \tag{43}$$

where

$\rho_{t,Y}$ is the transverse relative radius of curvature [see Formula (41)];

β_b is the base helix angle.

11 Load sharing factor, X_Y

11.1 General

The load sharing factor, X_Y, accounts for the load sharing of succeeding pairs of meshing teeth. The load sharing factor is presented as a function of the linear parameter, g_Y, on the path of contact[4] [see Formulae (44) to (59)].

Due to inaccuracies, a preceding pair of meshing teeth can cause an instantaneous increase or decrease of the theoretical load sharing factor, independent of the instantaneous increase or decrease caused by inaccuracies of a succeeding pair of meshing teeth at a later time. The value of X_Y does not exceed 1,0 (for cylindrical gears), which means full transverse single tooth contact. The region of transverse single tooth contact can be extended by an irregularly varying location of a dynamic load.

The load sharing factor, X_Y, depends on the type of gear transmission and on the profile modification. In case of buttressing of helical teeth (no profile modification), the load sharing factor is combined with a buttressing factor, $X_{but,Y}$[4].

11.2 Spur gears with unmodified profiles

The load sharing factor for a spur gear with unmodified profile is conventionally supposed to have a discontinuous trapezoidal shape (see Figure 2). However, due to manufacturing inaccuracies, in each path of double contact the load sharing factor will increase for protruding flanks and decrease for other flanks. The representative load sharing factor is an envelope of possible curves (see Figure 3).

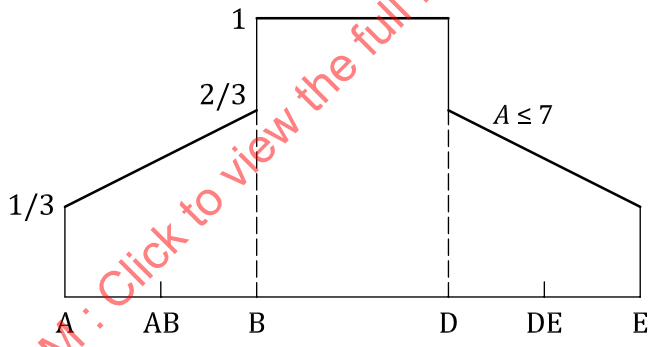

Figure 2 — Load sharing factor for cylindrical spur gears with unmodified profiles and tolerance class ≤ 7

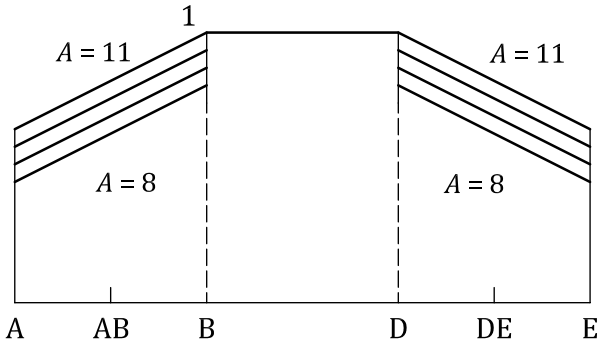

Figure 3 — Load sharing factor for cylindrical spur gears with unmodified profiles and tolerance class ≥ 8

$$X_Y = \frac{A-2}{15} + \frac{1}{3} \cdot \frac{g_Y}{g_B} \qquad \text{for } g_A \le g_Y < g_B \tag{44}$$

$$X_Y = 1{,}0 \qquad \text{for } g_B \le g_Y \le g_D \tag{45}$$

$$X_Y = \frac{A-2}{15} + \frac{1}{3} \cdot \frac{g_\alpha - g_Y}{g_\alpha - g_D} \qquad \text{for } g_D < g_Y \le g_E \tag{46}$$

where

$A = 7$ for tolerance class ≤ 7;

A is equal to the tolerance class for class ≥ 8.

11.3 Spur gears with profile modification

For load sharing factor for cylindrical spur gears with adequate profile modification on pinion and wheel, see Figure 4.

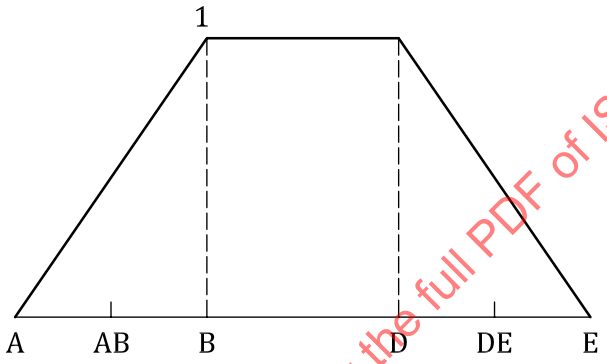

Figure 4 — Load sharing factor for cylindrical spur gears with adequate profile modification

$$X_Y = \frac{g_Y}{g_B} \qquad \text{for } g_A \le g_Y \le g_B \tag{47}$$

$$X_Y = 1{,}0 \qquad \text{for } g_B < g_Y < g_D \tag{48}$$

$$X_Y = \frac{g_\alpha - g_Y}{g_\alpha - g_D} \qquad \text{for } g_D \le g_Y \le g_E \tag{49}$$

For load sharing factor for cylindrical spur gears with adequate profile modifications on the addendum of the wheel and/or the dedendum of the pinion, see Figure 5.

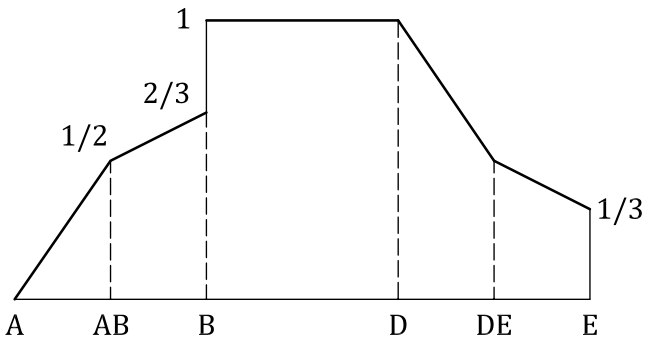

Figure 5 — Load sharing factor for cylindrical spur gears with adequate profile modification on the addendum of the wheel and/or the dedendum of the pinion

$$X_Y = \frac{g_Y}{g_B} \quad \text{for } g_A \le g_Y \le g_{AB} \tag{50}$$

$$X_Y = \frac{1}{3} + \frac{1}{3} \cdot \frac{g_Y}{g_B} \quad \text{for } g_{AB} < g_Y < g_B \tag{51}$$

$$X_Y = 1{,}0 \quad \text{for } g_B \le g_Y < g_D \tag{52}$$

$$X_Y = \frac{g_\alpha - g_Y}{g_\alpha - g_D} \quad \text{for } g_D \le g_Y \le g_{DE} \tag{53}$$

$$X_Y = \frac{1}{3} + \frac{1}{3} \cdot \frac{g_\alpha - g_Y}{g_\alpha - g_D} \quad \text{for } g_{DE} < g_Y \le g_E \tag{54}$$

For load sharing factor for cylindrical spur gears with adequate profile modifications on the addendum of the pinion and/or the dedendum of the wheel, see Figure 6.

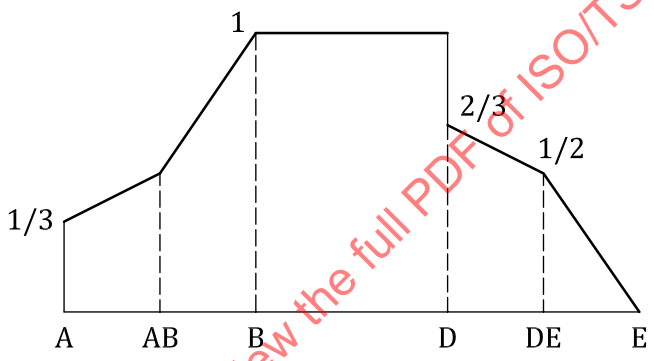

Figure 6 — Load sharing factor for cylindrical spur gears with adequate profile modification on the addendum of the pinion and/or the dedendum of the wheel

$$X_Y = \frac{1}{3} + \frac{1}{3} \cdot \frac{g_Y}{g_B} \quad \text{for } g_A \le g_Y \le g_{AB} \tag{55}$$

$$X_Y = \frac{g_Y}{g_B} \quad \text{for } g_{AB} < g_Y \le g_B \tag{56}$$

$$X_Y = 1{,}0 \quad \text{for } g_B < g_Y \le g_D \tag{57}$$

$$X_Y = \frac{1}{3} + \frac{1}{3} \cdot \frac{g_\alpha - g_Y}{g_\alpha - g_D} \quad \text{for } g_D < g_Y \le g_{DE} \tag{58}$$

$$X_Y = \frac{g_\alpha - g_Y}{g_\alpha - g_D} \quad \text{for } g_{DE} < g_Y \le g_E \tag{59}$$

11.4 Local buttressing factor, $X_{but,Y}$

Helical gears can have a buttressing effect near the end points A and E of the path of contact, due to the oblique contact lines. This applies to cylindrical helical gears with no profile modification.

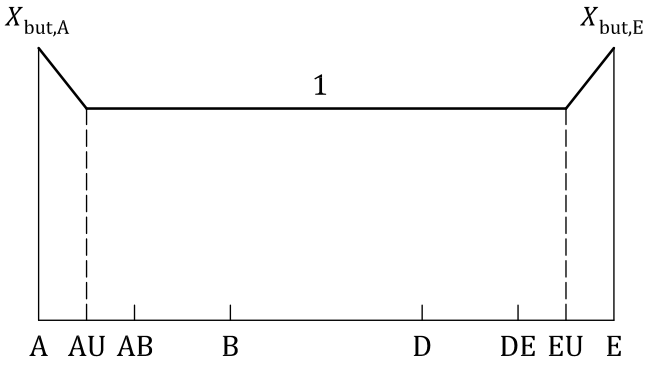

Figure 7 — Local buttressing factor, $X_{but,Y}$

The buttressing is expressed by means of a factor $X_{but,Y}$ (see Figure 7), marked by the values in Formulae (60) to (66):

$$g_{AU} - g_A = g_E - g_{EU} = C \cdot \sin\beta_b \tag{60}$$

where

g_A = 0 mm;

g_E = g_α (see Figure 1).

$$X_{but,A} = X_{but,E} = 1{,}3 \qquad \text{if } \varepsilon_\beta \geq 1{,}0 \tag{61}$$

$$X_{but,A} = X_{but,E} = 1 + 0{,}3 \cdot \varepsilon_\beta \qquad \text{if } \varepsilon_\beta < 1{,}0 \tag{62}$$

$$X_{but,AU} = X_{but,EU} = 1{,}0 \tag{63}$$

$$X_{but,Y} = X_{but,A} - \frac{g_Y}{C \cdot \sin\beta_b} \cdot \left(X_{but,A} - 1\right) \qquad \text{for } g_A \leq g_Y < g_{AU} \tag{64}$$

$$X_{but,Y} = 1{,}0 \qquad \text{for } g_{AU} \leq g_Y \leq g_{EU} \tag{65}$$

$$X_{but,Y} = X_{but,E} - \frac{g_\alpha - g_Y}{C \cdot \sin\beta_b} \cdot \left(X_{but,E} - 1\right) \qquad \text{for } g_{EU} < g_Y \leq g_E \tag{66}$$

where

C = 0,2 mm;

ε_β is the overlap ratio.

11.5 Helical gears with $\varepsilon_\beta \leq 0{,}8$ and unmodified profiles

Helical gears with a transverse contact ratio $\varepsilon_\alpha \geq 1$ and overlap ratio $\varepsilon_\beta \leq 0{,}8$, have poor single contact of tooth pairs. Hence, they can be treated similar to spur gears, considering the geometry in the transverse plane, as well as the buttressing effect (see Figure 8).

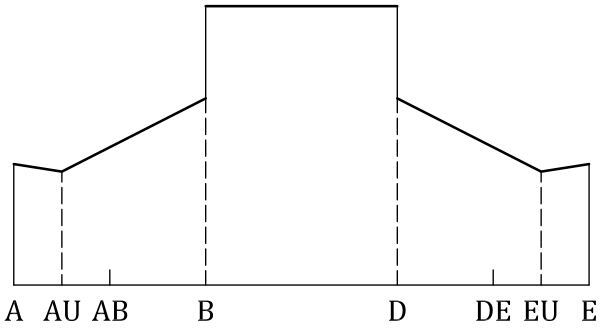

Figure 8 — Load sharing factor of cylindrical helical gears with $\varepsilon_\beta \leq 0{,}8$ and unmodified profiles, including the buttressing effect

The load sharing factor is obtained by multiplying the X_Y in 11.2 with the buttressing factor, $X_{but,Y}$, in 11.4.

11.6 Helical gears with $\varepsilon_\beta \leq 0{,}8$ and profile modification

Helical gears with a transverse contact ratio $\varepsilon_\alpha \geq 1$ and overlap ratio $\varepsilon_\beta \leq 0{,}8$, have poor single contact of tooth pairs. Hence, they can be treated similar to spur gears, considering the geometry in the transverse plane (see Figures 9 to 11).

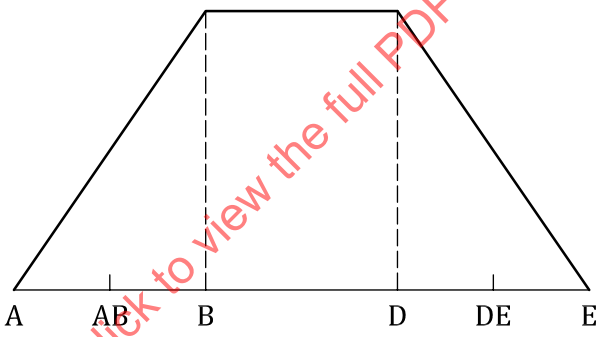

Figure 9 — Load sharing factor for cylindrical helical gears with $\varepsilon_\beta \leq 0{,}8$ and adequate profile modification

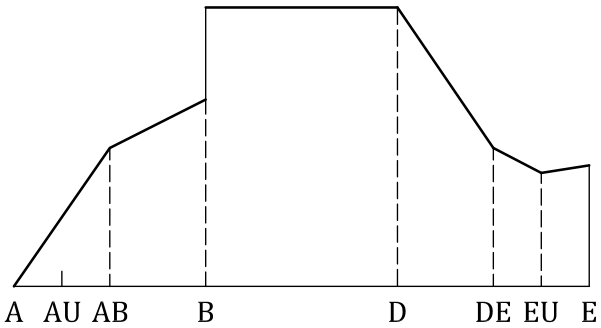

Figure 10 — Load sharing factor for cylindrical helical gears with $\varepsilon_\beta \leq 0{,}8$ and adequate profile modification on the addendum of the wheel and/or the dedendum of the pinion

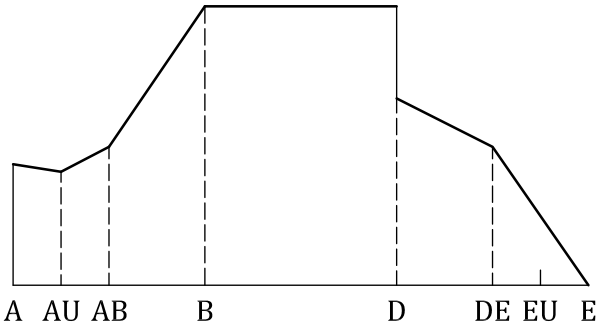

Figure 11 — Load sharing factor for cylindrical helical gears with $\varepsilon_\beta \leq 0{,}8$ and adequate profile modification on the addendum of the pinion and/or the dedendum of the wheel

The load sharing factor is obtained by multiplying the X_Y in 11.3 with the buttressing factor, $X_{but,Y}$, in 11.4.

11.7 Helical gears with $\varepsilon_\beta \geq 1{,}2$ and unmodified profiles

The buttressing effect of local high mesh stiffness at the end of oblique contact lines for helical gears with $\varepsilon_\alpha \geq 1$ and $\varepsilon_\beta \geq 1{,}2$, is assumed to act near the ends A and E along the helix teeth over a constant length, which corresponds to a transverse relative distance 0,2 mm · $\sin\beta_b$ (see Figure 12; see also 11.3 and Figure 7).

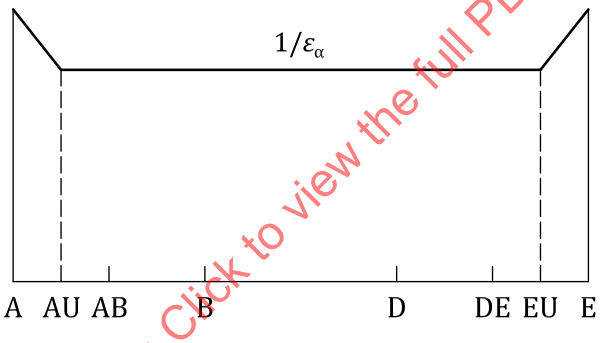

Figure 12 — Load sharing factor for cylindrical helical gears with $\varepsilon_\beta \geq 1{,}2$ and unmodified profiles

As shown in Formula (67), the load sharing factor is obtained by multiplying the value $1/\varepsilon_\alpha$, representing the mean load, with the buttressing factor, $X_{but,Y}$:

$$X_Y = \frac{1}{\varepsilon_\alpha} \cdot X_{but,Y} \tag{67}$$

where ε_α is the transverse contact ratio.

11.8 Helical gears with $\varepsilon_\beta \geq 1{,}2$ and profile modification

Tip relief on the pinion (respectively wheel) reduces X_Y in the range DE-E (respectively A-AB) and increases X_Y in the range AB-DE [see Figures 13 to 15 and Formulae (68) to (76)]. The extensions of tip relief at both ends A-AB and DE-E of the path of contact are assumed to be equal and to result in a contact ratio $\varepsilon_\alpha = 1$ for unloaded gears (see Figure 13).

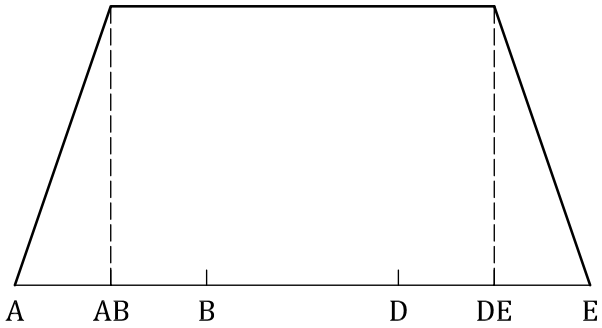

Figure 13 — Load sharing factor for cylindrical helical gears with $\varepsilon_\beta \geq 1{,}2$ and adequate profile modification

$$X_Y = \left[\frac{1}{\varepsilon_\alpha} + \frac{(\varepsilon_\alpha - 1)}{\varepsilon_\alpha \cdot (\varepsilon_\alpha + 1)}\right] \cdot \frac{g_Y}{g_{AB}} \qquad \text{for } g_A \leq g_Y < g_{AB} \tag{68}$$

$$X_Y = \frac{1}{\varepsilon_\alpha} + \frac{(\varepsilon_\alpha - 1)}{\varepsilon_\alpha \cdot (\varepsilon_\alpha + 1)} \qquad \text{for } g_{AB} < g_Y \leq g_{DE} \tag{69}$$

$$X_Y = \left[\frac{1}{\varepsilon_\alpha} \cdot \frac{(\varepsilon_\alpha - 1)}{\varepsilon_\alpha \cdot (\varepsilon_\alpha + 1)}\right] \cdot \frac{g_\alpha - g_Y}{g_\alpha - g_{DE}} \qquad \text{for } g_{DE} < g_Y \leq g_E \tag{70}$$

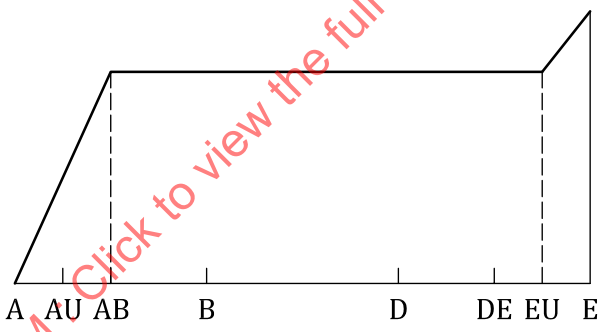

Figure 14 — Load sharing factor for cylindrical helical gears with $\varepsilon_\beta \geq 1{,}2$ and adequate profile modification on the addendum of the wheel and/or the dedendum of the pinion

$$X_Y = \left[\frac{1}{\varepsilon_\alpha} + \frac{(\varepsilon_\alpha - 1)}{2 \cdot \varepsilon_\alpha \cdot (\varepsilon_\alpha + 1)}\right] \cdot \frac{g_Y}{g_{AB}} \qquad \text{for } g_A \leq g_Y \leq g_{AB} \tag{71}$$

$$X_Y = \frac{1}{\varepsilon_\alpha} + \frac{(\varepsilon_\alpha - 1)}{2 \cdot \varepsilon_\alpha \cdot (\varepsilon_\alpha + 1)} \qquad \text{for } g_{AB} < g_Y \leq g_{EU} \tag{72}$$

$$X_Y = \left[\frac{1}{\varepsilon_\alpha} \cdot \frac{(\varepsilon_\alpha - 1)}{2 \cdot \varepsilon_\alpha \cdot (\varepsilon_\alpha + 1)}\right] \cdot X_{but,Y} \qquad \text{for } g_{EU} < g_Y \leq g_E \tag{73}$$

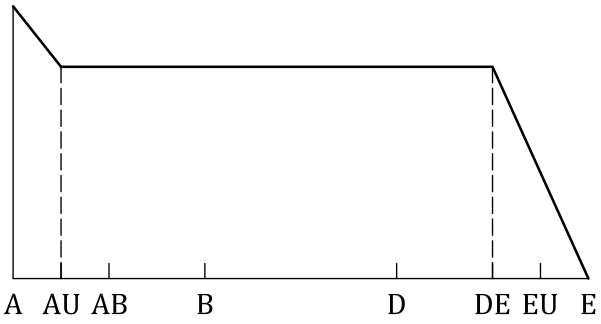

Figure 15 — Load sharing factor for cylindrical helical gears with $\varepsilon_\beta \geq 1{,}2$ and adequate profile modification on the addendum of the pinion and/or the dedendum of the wheel

$$X_Y = \left[\frac{1}{\varepsilon_\alpha} \cdot \frac{(\varepsilon_\alpha - 1)}{2 \cdot \varepsilon_\alpha \cdot (\varepsilon_\alpha + 1)}\right] \cdot X_{\text{but,Y}} \qquad \text{for } g_A \leq g_Y \leq g_{AU} \tag{74}$$

$$X_Y = \frac{1}{\varepsilon_\alpha} + \frac{(\varepsilon_\alpha - 1)}{2 \cdot \varepsilon_\alpha \cdot (\varepsilon_\alpha + 1)} \qquad \text{for } g_{AU} < g_Y \leq g_{DE} \tag{75}$$

$$X_Y = \left[\frac{1}{\varepsilon_\alpha} \cdot \frac{(\varepsilon_\alpha - 1)}{2 \cdot \varepsilon_\alpha \cdot (\varepsilon_\alpha + 1)}\right] \frac{g_\alpha - g_Y}{g_\alpha - g_{DE}} \qquad \text{for } g_{DE} < g_Y \leq g_E \tag{76}$$

11.9 Helical gears with $0{,}8 < \varepsilon_\beta < 1{,}2$

Due to the fact that gears are not infinitely stiff, the overlap ratio changes depending on the load. To take this into account, for helical gears with calculated overlap ratios of $0{,}8 < \varepsilon_\beta < 1{,}2$, an interpolation between the load sharing factor $X_Y(\varepsilon_\beta = 0{,}8)$ for $\varepsilon_\beta = 0{,}8$ (see 11.5 for unmodified profiles or 11.6 for modified profiles) and $X_Y(\varepsilon_\beta = 1{,}2)$ for $\varepsilon_\beta = 1{,}2$ (see 11.7 for unmodified profiles or 11.8 for modified profiles) shall be performed. For helical gears with $0{,}8 < \varepsilon_\beta < 1{,}2$, X_Y is calculated with Formula (77):

$$X_Y(\varepsilon_\beta) = X_Y(\varepsilon_\beta = 0{,}8) \cdot \frac{1{,}2 - \varepsilon_\beta}{0{,}4} + X_Y(\varepsilon_\beta = 1{,}2) \cdot \frac{\varepsilon_\beta - 0{,}8}{0{,}4} \tag{77}$$

12 Local contact temperature, $\theta_{B,Y}$

The local contact temperature, $\theta_{B,Y}$, calculated with Formula (78), is defined as the sum of bulk temperature θ_M and local flash temperature, $\theta_{fl,Y}$ (see also ISO/TS 6336-20 and ISO/TS 6336-21). As a result of friction in the tooth mesh, the flash temperature, $\theta_{fl,Y}$, varies along the path of contact. Hence, the local flash temperature, $\theta_{fl,Y}$, shall be determined for every desired point Y in the field of contact. For simplification, the bulk temperature, θ_M, is assumed as constant.

$$\theta_{B,Y} = \theta_M + \theta_{fl,Y} \tag{78}$$

where

$\theta_{fl,Y}$ is the local flash temperature (see Clause 13);

θ_M is the bulk temperature (see Clause 14).

13 Local flash temperature, $\theta_{fl,Y}$

The local flash temperature, $\theta_{fl,Y}$, of the gear flanks is rapidly fluctuating in contact. In every mesh position, different rolling and sliding conditions occur. Furthermore, the local contact load varies along

the path of contact. These conditions cause a continuous variation of the flash temperature which can be calculated according to Blok[13] by Formulae (79) to (82).

$$\theta_{\mathrm{fl,Y}} = \frac{\sqrt{\pi}}{2} \cdot \frac{\mu_{\mathrm{m}} \cdot p_{\mathrm{dyn,Y}} \cdot 10^{6} \cdot \left| v_{\mathrm{g,Y}} \right|}{B_{\mathrm{M1}} \cdot \sqrt{v_{\mathrm{r1,Y}}} + B_{\mathrm{M2}} \cdot \sqrt{v_{\mathrm{r2,Y}}}} \cdot \sqrt{8 \cdot \rho_{\mathrm{n,Y}} \cdot \frac{p_{\mathrm{dyn,Y}}}{1\,000 \cdot E_{\mathrm{r}}}} \tag{79}$$

where

$$v_{\mathrm{g,Y}} = v_{\mathrm{r1,Y}} - v_{\mathrm{r2,Y}} \tag{80}$$

$$B_{\mathrm{M1}} = \sqrt{\rho_{\mathrm{M1}} \cdot c_{\mathrm{M1}} \cdot \lambda_{\mathrm{M1}}} \tag{81}$$

$$B_{\mathrm{M2}} = \sqrt{\rho_{\mathrm{M2}} \cdot c_{\mathrm{M2}} \cdot \lambda_{\mathrm{M2}}} \tag{82}$$

$v_{\mathrm{g,Y}}$ is the local sliding velocity;

B_{M1} is the thermal contact coefficient of pinion (see Table 3);

B_{M2} is the thermal contact coefficient of wheel (see Table 3);

μ_{m} is the mean coefficient of friction (see 14.2);

$p_{\mathrm{dyn,Y}}$ is the local Hertzian contact stress (see 8.2 and 8.3);

$v_{\mathrm{r1,Y}}$ is the local tangential velocity on pinion (see 7.2);

$v_{\mathrm{r2,Y}}$ is the local tangential velocity on wheel (see 7.2);

$\rho_{\mathrm{n,Y}}$ is the local normal radius of relative curvature (see Clause 10);

E_{r} is the reduced modulus of elasticity (see 6.2).

Table 3 — Material properties of steel

Material	Density ρ_{M} kg/m³	Specific heat capacity c_{M} J/(kg·K)	Specific heat conductivity λ_{M} W/(m·K)
Steel	7 800	440	45

14 Bulk temperature, θ_{M}

14.1 General

The bulk temperature, θ_{M}, is the equilibrium temperature of the surface of the gear teeth before they enter the contact zone. The bulk temperature, θ_{M}, should be measured or calculated by an adequate method. If this is not possible, θ_{M} can be approximated according to Formulae (83) and (84) (see [9]).

$$\theta_{\mathrm{M}} = \theta_{\mathrm{oil}} + 7\,400 \cdot \left(\frac{P \cdot \mu_{\mathrm{m}} \cdot H_{\mathrm{v}}}{a \cdot b} \right)^{0,72} \cdot \frac{X_{\mathrm{S}}}{1,2 \cdot X_{\mathrm{Ca}}} \tag{83}$$

where

$$P = 2 \cdot \grave{\mathrm{A}} \cdot \frac{n_1}{60} \cdot \frac{T_1}{1\,000} \tag{84}$$

P is the transmitted power;

a is the centre distance;

b is the face width;

θ_{oil} is the lubricant inlet or oil sump temperature;

θ_m is the mean coefficient of friction (see 14.2);

H_v is the load losses factor (see 14.3);

X_{Ca} is the tip relief factor (see 14.4);

X_S is the lubrication factor (see 14.5);

n_1 is the rotational speed of pinion;

T_1 is the nominal torque at the pinion.

NOTE If the calculated pitch line velocity exceeds 80 m/s, refer to the scope.

14.2 Mean coefficient of friction, μ_m

The mean coefficient of friction, μ_m, depends on the gear geometry, the surface roughness, the tangential velocity, the tangential load and the dynamic viscosity of the lubricant. It can be approximated by Formulae (85) and (86):

$$\mu_m = 0{,}045 \cdot \left(\frac{K_A \cdot K_v \cdot K_{H\alpha} \cdot K_{H\beta} \cdot F_{bt} \cdot K_{B\gamma}}{b \cdot v_{\Sigma,C} \cdot \rho_{n,C}} \right)^{0,2} \cdot \left(10^3 \cdot \eta_{\theta oil}\right)^{-0,05} \cdot X_R \cdot X_L \quad (85)$$

where

$$X_R = 2{,}2 \cdot \left(\frac{Ra}{\rho_{n,C}} \right)^{0,25} \quad (86)$$

X_R is the roughness factor according to ISO/TS 6336-21;

b is the face width;

F_{bt} is the nominal transverse load in plane of action;

K_A is the application factor (according to ISO 6336-1);

$K_{B\gamma}$ is the helical load factor (see below);

$K_{H\alpha}$ is the transverse load factor (according to ISO 6336-1);

$K_{H\beta}$ is the face load factor (according to ISO 6336-1);

K_v is the dynamic factor (according to ISO 6336-1);

$v_{\Sigma,C}$ is the sum of the tangential velocities at the pitch point (see 7.2);

$\eta_{\theta oil}$ is the dynamic viscosity at inlet or oil sump temperature;

$\rho_{n,C}$ is the normal radius of relative curvature at the pitch diameter;

Ra is the effective arithmetic mean roughness value (see 5.3);

X_L is the lubricant factor (see Table 4).

The helical load factor, $K_{B\gamma}$, calculated with Formulae (87) to (89), takes into account an increasing friction for increasing total contact ratio (see Figure 16)

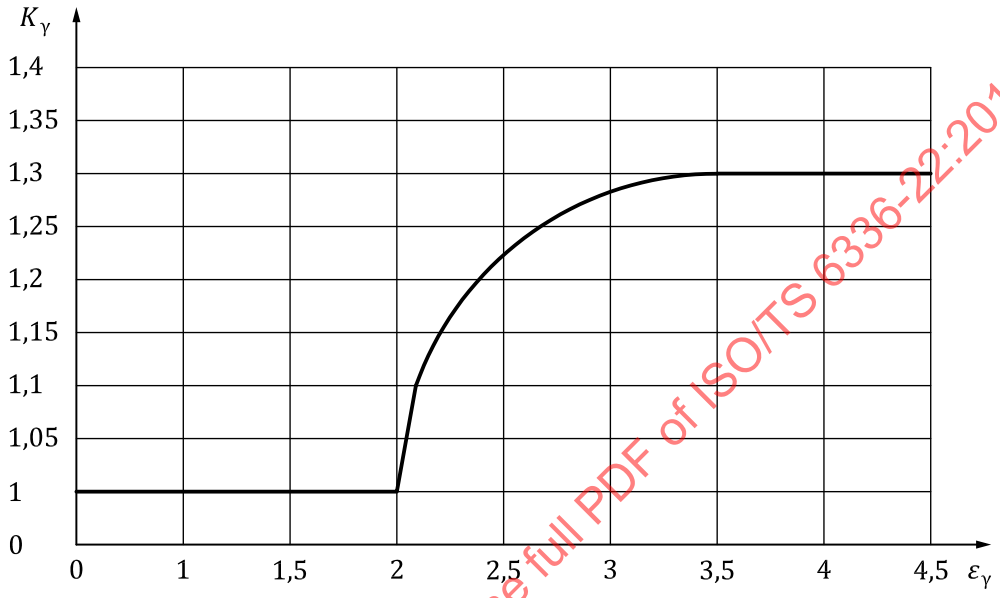

Key

ε_γ total contact ratio

Figure 16 — Helical load factor, $K_{B\gamma}$

$$K_{B\gamma} = 1,0 \qquad \text{if } \varepsilon_\gamma \le 2 \tag{87}$$

$$K_{B\gamma} = 1 + 0,2 \cdot \sqrt{(\varepsilon_\gamma - 2)\cdot(5 - \varepsilon_\gamma)} \qquad \text{if } 2 < \varepsilon_\gamma < 3,5 \tag{88}$$

$$K_{B\gamma} = 1,3 \qquad \text{if } \varepsilon_\gamma \ge 3,5 \tag{89}$$

Table 4 — Lubricant factor, X_L

Oil type	X_L
Mineral oil	1,0
Polyalfaolefin	0,8
Non water-soluble polyglycols	0,7
Water-soluble polyglycols	0,6
Traction fluid	1,5
Phosphate ester	1,3

14.3 Load losses factor, H_v

The load losses factor, H_v, is calculated according to Formulae (90) and (91):

$$H_v = \left(\varepsilon_1^2 + \varepsilon_2^2 + 1 - \varepsilon_\alpha\right) \cdot \left(\frac{1}{z_1} + \frac{1}{z_2}\right) \cdot \frac{\pi}{\cos\beta_b} \qquad \text{if } \varepsilon_\alpha < 2 \tag{90}$$

$$H_v = 0{,}5 \cdot \varepsilon_\alpha \cdot \left(\frac{1}{z_1} + \frac{1}{z_2}\right) \cdot \frac{\pi}{\cos\beta_b} \qquad \text{if } \varepsilon_\alpha \geq 2 \tag{91}$$

where

z_1 is the number of teeth of pinion;

z_2 is the number of teeth of wheel;

β_b is the base helix angle

ε_1 is the addendum contact ratio of the pinion;

ε_2 is the addendum contact ratio of the wheel;

ε_α is the transverse contact ratio.

14.4 Tip relief factor, X_{Ca}

The elastic deformation of the meshing teeth results in overload on the tip in the area of high sliding. The tip relief factor, X_{Ca}, according to Figure 17 and Figure 18, considers the positive influence of the profile modification on this overload.

The tip relief factor applies to gears of ISO tolerance class ≤6, in accordance with ISO 1328-1. For less accurate gears, X_{Ca} is to be set at 1 (see also ISO 6336-1).

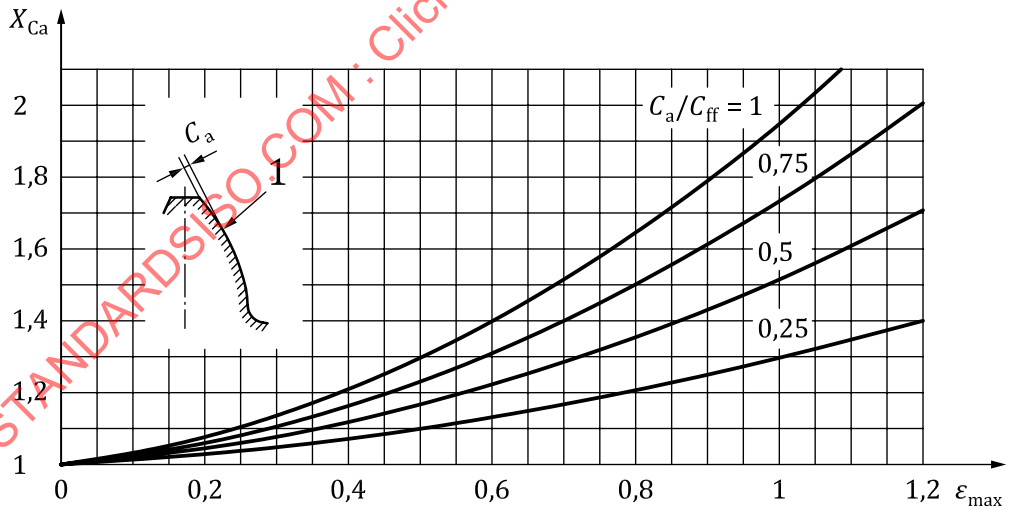

Key

1 upper point of single pair tooth contact

ε_{max} greater value of ε_1 and ε_2

Figure 17 — Tip relief factor, X_{Ca}, according to method A